The ISME Journal (2014) 8, 1069–1078

www.nature.com/ismej

ORIGINAL ARTICLE

Methanotrophic archaea possessing diverging methane-oxidizing and electron-transporting pathways

Feng-Ping Wang[1,2,3,7], Yu Zhang[1,2,4,7], Ying Chen[1], Ying He[1], Ji Qi[5], Kai-Uwe Hinrichs[6], Xin-Xu Zhang[1], Xiang Xiao[1,2] and Nico Boon[4]

[1]*State Key Laboratory of Microbial Metabolism, School of Life Sciences and Biotechnology, Shanghai Jiao Tong University, Shanghai, People's Republic of China;* [2]*State Key Laboratory of Ocean Engineering, School of Naval Architecture, Ocean and Civil Engineering, Shanghai Jiao Tong University, Shanghai, People's Republic of China;* [3]*Key Laboratory of Systems Biomedicine (Ministry of Education), School of Systems Biomedicine, Shanghai Jiao Tong University, Shanghai, People's Republic of China;* [4]*Laboratory of Microbial Ecology and Technology (LabMET), Ghent University, Gent, Belgium;* [5]*School of Life Sciences, Fu Dan University, Shanghai, People's Republic of China and* [6]*MARUM Center for Marine Environmental Sciences and Department of Geosciences, University of Bremen, Bremen, Germany*

Anaerobic oxidation of methane (AOM) is a crucial process limiting the flux of methane from marine environments to the atmosphere. The process is thought to be mediated by three groups of uncultivated methane-oxidizing archaea (ANME-1, 2 and 3). Although the responsible microbes have been intensively studied for more than a decade, central mechanistic details remain unresolved. On the basis of an integrated analysis of both environmental metatranscriptome and single-aggregate genome of a highly active AOM enrichment dominated by ANME-2a, we provide evidence for a complete and functioning AOM pathway in ANME-2a. All genes required for performing the seven steps of methanogenesis from CO_2 were found present and actively expressed. Meanwhile, genes for energy conservation and electron transportation including those encoding $F_{420}H_2$ dehydrogenase (Fpo), the cytoplasmic and membrane-associated Coenzyme B–Coenzyme M heterodisulfide (CoB-S-SCoM) reductase (HdrABC, HdrDE), cytochrome *C* and the Rhodobacter nitrogen fixation (Rnf) complex were identified and expressed, whereas genes encoding for hydrogenases were absent. Thus, ANME-2a is likely performing AOM through a complete reversal of methanogenesis from CO_2 reduction without involvement of canonical hydrogenase. ANME-2a is demonstrated to possess versatile electron transfer pathways that would provide the organism with more flexibility in substrate utilization and capacity for rapid adjustment to fluctuating environments. This work lays the foundation for understanding the environmental niche differentiation, physiology and evolution of different ANME subgroups.

The ISME Journal (2014) **8,** 1069–1078; doi:10.1038/ismej.2013.212; published online 12 December 2013
Subject Category: Integrated genomics and post-genomics approaches in microbial ecology
Keywords: methane oxidation; electron transportation; single aggregate genome; metatranscriptome; methanogenesis

Introduction

Anaerobic oxidization of methane (AOM) coupled to sulfate reduction is a key process that effectively controls the methane emission from anoxic marine waters and sediments to the oxygenated ocean (Reeburgh, 1976, 2007). The microorganisms thought to be mediating AOM have been designated as anaerobic methane-oxidizing archaea (ANME), close phylogenetic relatives of the methanogenic archaea. These microorganisms consist of three established groups (ANME-1, ANME-2 and ANME-3) that can form syntrophic aggregates with sulfate-reducing bacteria (SRB) or exist as single cells (Hinrichs *et al.*, 1999; Boetius *et al.*, 2000; Orphan *et al.*, 2001; Knittel and Boetius, 2009). AOM has been hypothesized to be operated via a reversal of the methanogenesis reaction (Hoehler *et al.*, 1994), and this hypothesis has been partly supported by metagenome-based analyses of communities dominated by ANME-1 (Hallam *et al.*, 2004; Meyerdierks *et al.*, 2010).

Correspondence: F-P Wang or X Xiao, School of Life Sciences and Biotechnology, Shanghai Jiao Tong University, 800 Dongchuan Road, Shanghai 200240, People's Republic of China.
E-mail: fengpingw@sjtu.edu.cn or xoxiang@sjtu.edu.cn
[7]These authors contributed equally to this work.
Received 6 June 2013; revised 26 September 2013; accepted 22 October 2013; published online 12 December 2013

However, the evidence remains inconclusive because one of the genes in canonical CO_2-dependent methanogenesis, the N^5,N^{10}-methylene-tetrahydromethanopterin (methylene-H_4MPT) reductase (Mer, which catalyzes the reaction from methylene-H_4MPT to methyl-H_4MPT) gene *mer*, has not been found in the metagenomes of ANME-1. Meanwhile, very limited genomic information is available for ANME-2 or ANME-3 (Hallam *et al.*, 2004; Pernthaler *et al.*, 2008; Stokke *et al.*, 2012). Consequently, it remains unresolved if and how the AOM pathway differs among the various ANME clades.

The available ANME metagenomes do not provide solid information about electron transport and energy conservation in reverse methanogenesis. A novel type of sulfate reduction has been recently recognized as electron sink to methane oxidation in an ANME-2 enrichment by generating the energy for ANME-2 with zero-valent sulfur being an intermediate then disproportionated by SRB cells (Milucka *et al.*, 2012). However, the intracellular electron transporting within ANME remains to be unveiled. AOM via the 'reverse methanogenesis hypothesis' requires the presence of genes for electron transport from the primary electron acceptors CoM-S-S-CoB (generated in the heterodisulfide reductase reaction), coenzyme F_{420} (generated in the methylene-H_4MPT reductase and methylene-H_4MPT dehydrogenase reactions) and ferredoxin (generated in the formylmethanofuran dehydrogenase reaction) to a terminal electron acceptor that has been proposed to be protons (Hoehler *et al.*, 1994; Thauer, 2011). All known methanogenic archaea require H_2 for CO_2 reduction. In the case of reverse methanogenesis with H_2 as a product, the presence of hydrogenases would be required. However, these hydrogenases have not been confirmed in the ANME-1 metagenome (Meyerdierks *et al.*, 2010).

Therefore, central mechanistic details on AOM remain unresolved such as whether 'reverse methanogenesis' properly describes the AOM mechanism, and how electrons are transferred within ANME. In this study, we try to address these gaps in knowledge through an integrated analysis of single-aggregate ANME-2a genome and its gene expression, to reveal the pathways for methane oxidation and energy transportation in ANME-2a.

Materials and methods

Origin of sample

Sediment samples from Capt Aryutinov Mud Volcano (coordinates: 35:39.700/07:20.012, Gulf of Cadiz, Atlantic Ocean, 1200 m water depth) were collected during a Maria S. Merian 1/3 cruise on 30 April 2006. After the activation of AOM activity at ambient pressure, a total volume of 600 ml diluted sediment slurry (1:12 w:w) was incubated into a special designed continuous high-pressure bioreactor under 8 MPa methane pressure at 15 °C for over 1 year. A highly enriched AOM culture was obtained, of which an approximate 0.5 mmol day^{-1} methane oxidation-dependent sulfate reduction rate has been measured (Zhang *et al.*, 2010, 2011). A well-mixed slurry sample (~120 ml) of this active enrichment was taken out and immediately fixed with RNAlater (Sigma-Aldrich, Munich, Germany) and stored at −80 °C before mRNA extraction for metatranscriptome analysis. From the same enrichment, a slurry sample was taken out directly without fixation for single-aggregate extraction and genome analysis.

RNA isolation and complementary DNA synthesis

RNA was isolated using the RNA isolation kit (Omega Bio-Tek, Doraville, GA, USA) following the user manual. DNA contamination was ruled out according to PCR results of the RNA sample where it was used as template and amplified with archaeal and bacterial 16S ribosomal RNA (rRNA) gene universal primers (Arch21F and Arch958R for archaea; Eubac27F and Eubac 1492R for bacteria; see Zhang *et al.*, 2011). The mRNA fraction was enriched by the enzymatic digestion of rRNA molecules (mRNA-ONLY Prokaryotic mRNA Isolation kit, Epicentre Biotechnologies, Madison, WI, USA) followed by subtractive hybridization of rRNA with capture oligonucleotides (Ambion MICROBExpress kit, Life Technologies, Gaithersburg, MD, USA). The mRNA isolates were amplified (MessageAmp II-Bacteria kit, Ambion, Life Technologies) and reversely transcribed into complementary DNA and then directly sequenced using the Illumina (Shenzhen, China) GAIIx platform for metatranscriptome analysis.

Sample preparation and single-aggregate extraction

Separation of cells from AOM enrichment was conducted using Percoll discontinuous density gradients (1.080, 1.069 and 1.060 g ml^{-1}) method. Enrichment was firstly sonicated on ice at an output power of 165 W for 30 s with 5 s pulse, and then overlaid on the top of the gradients to centrifuge at 1000 *g* for 2 h. The total supernatant from gradients was filtered through a 3-μm pore-size polycarbonate filter that was subsequently washed twice with phosphate-buffered saline to remove any trace Percoll and afterwards suspended into 1 ml phosphate-buffered saline solution. From the cell suspension, 500 μl was transferred onto an adhesion slide and incubated inside a moist chamber. After 10 min of sedimentation, most of the cells and aggregates were fixed onto the surface of the slide. In the light field of microscope, aggregates were captured with a capillary glass micropipette (with an inner diameter of 8 μm, prepared with Micropipette Puller system P-2000, Sutter Instrument Company, Los Angeles, CA, USA) using a XenoWorks Microinjection System (Sutter Instrument Company). The captured

aggregates were transferred into sterile 0.2 ml tubes that were pre-filled with 3.5 μl of phosphate-buffered saline. Each tube contained one aggregate. These aggregate samples were immediately stored at −70 °C for further characterization.

Whole-genome amplification

Whole-genome multiple displacement amplification (MDA) on single aggregate was conducted by REPLI-g Mini kit reagents (Qiagen, Hilden, Germany) following the manufacturer's protocol. DNA (500–800 ng) was generated after each MDA reaction and the first-round MDA product was used for 16S rRNA gene characterization. Forward primer Arch21F (Delong, 1992) and three reverse primers ANME-2-538 (Treude *et al.*, 2005), Arch915 (Stahl and Amann, 1991) and Arch958 (Delong, 1992) were applied for archaeal 16S rRNA gene amplification. The bacterial 16S rRNA gene fragments were amplified with the primer set of Bac27F and Bac1492R. The PCR was initiated with a denaturing step at 94 °C for 2 min. A total of 35 cycles of 30 s, 94 °C; 30 s, 55 °C; and 30 s, 72 °C (60 s for bacteria) were used for the PCR, and the reaction was terminated after 7 min of elongation. A second-round MDA was performed to meet the requirements of Illumina genome sequencing. During the second-round MDA, five parallel running of amplification reaction was performed for each sample to minimize stochastic bias. For each reaction, 5 μl of purified first-round MDA products was used as template. Amplified DNA products from all five reactions were pooled together and purified using QiaAmp DNA mini kit (Qiagen) following the manufacturer's protocol.

Genome sequencing, assembly, annotation and taxonomic assignment

Sequencing libraries (500 bp and 2 kbp) of the single-aggregate samples (second-round MDA products) were sequenced using the Illumina GAIIx 2×90 bp pair-end technology. Assembly of the Illumina reads was performed with SOAPdenovo 1.05 software (Li *et al.*, 2009). Gene prediction was carried out by using Glimmer3 software (Delcher *et al.*, 2007). Ribosomal RNA genes were detected by using the rRNA prediction algorithm (Huang *et al.*, 2009). For each predicted open reading frame, functional information was retrieved from the National Center for Biotechnology Information (NCBI) non-redundant (NR) database using blastx (Altschul *et al.*, 1997) with an *E*-value cutoff of $<10^{-5}$. Those sequences that had reliable hits from NR database were searched against the Kyoto Encyclopedia of Genes and Genomes (KEGG; Ogata *et al.*, 1999) database as well as the database for Clusters of Orthologous Groups of proteins database (COG; Tatusov *et al.*, 2000) (*E*-value cutoff of $<10^{-5}$) for functional annotation. To analyze the taxonomic contents, blastx results of all predicted gene features were visualized in MEGAN (Huson *et al.*, 2007). Each predicted gene feature in the single aggregate genome was assigned to a certain taxon when at least 75% of the BLAST hits of this query were from that specific taxon. Raw sequence data of the metatranscriptome and the single-aggregate genome have been submitted to the NCBI Sequence Read Archive under accessions SRX359351 and SRX359142, respectively. The assembled genome sequences of M25 have been incorporated into the Integrated Microbial Genomes (IMG) system with the ER submission ID 20381.

Phylogenetic tree construction

For phylogenetic analyses, multiple sequence alignments were conducted with CLUSTALW2 (Larkin *et al.*, 2007), and all phylogenetic trees were constructed by PhyML (Guindon and Gascuel, 2003). The LG (La Guscuel) substitution model was used for all the amino acid sequence-based phylogenies. Bootstrap values were obtained from 1000 replicates.

Estimation of complete genome size of ANME-2a

Genome size of ANME-2a was estimated based on a conserved single copy gene (CSCG) analysis (Woyke *et al.*, 2009). Here, genes from a single aggregate (where the only detected 16S rRNA gene belonged to ANME-2a) were used as a pool for CSCG detection. To identify relevant CSCGs for ANME-2a, 16 finished *Methanomicrobia* genomes (Supplementary Table S1) available in July 2012 at the IMG site (Markowitz *et al.*, 2012) were analyzed. COG distribution for the 16 analyzed genomes were retrieved from IMG and used for CSCG identification. The number of CSCGs (designated as C_n when shared by n genomes) was plotted against the number of genomes (n) and a power function fit was applied to the data. A regression curve was drawn to predict the number of CSCGs (C_{n+1}) remaining after adding one more genome ($n+1$). G_{n+1} presented the number of CSCGs on the assembly of the single-aggregate genome. The expected complete genome size of ANME-2 was estimated as described previously (Woyke *et al.*, 2009): $\mathrm{GS} = \mathrm{Co} \times \mathrm{AS}/\mathrm{RCSCG}$, where GS is the expected complete genome size; AS is the size of current genome assembly; RCSCG is the recovery of CSCGs ($\mathrm{RCSCG} = G_{n+1}/C_n$); Co is the correction coefficient to compensate for the expected lower number of CSCGs shared by $n+1$ genomes relative to n genomes ($\mathrm{Co} = C_{n+1}/C_n$).

Metatranscriptome sequencing, assembly and annotation

All metatranscriptomic reads were first aligned to a ribosome RNA database SILVA (Pruesse *et al.*, 2007) using blastn (*E*-value $<10^{-10}$). Only those

non-rRNA reads were included in further analysis and assembled using SOAP alignment software (Li *et al.*, 2009). Open reading frames were predicted with MetaGene Annotator (Noguchi *et al.*, 2008) and compared with the NCBI NR database using blastx with an *E*-value cutoff of $<10^{-5}$. Those sequences that had reliable hits from NR database were compared with the KEGG and COG databases (with *E*-value $<10^{-5}$) for functional annotation.

Estimation of gene expression in single-aggregate genome from metatranscriptomic transcripts

Metatranscriptomic reads were assigned to single-aggregate genes by blastx with *E*-value cutoff 10^{-10} and >90% identity, and then subject to manual inspection to ensure exact mappings between single-aggregate genes and their assigned metatranscriptomic reads. The expression level of each transcript in the transcriptome was quantified by RPKM (reads per Kb per million reads) to measure the read density, which reflected the molar concentration of a transcript in the starting sample by normalizing for RNA length and for the total read number in the measurement (Mortazavi *et al.*, 2008). This approach facilitated comparisons of transcript levels both within and between samples. The expression levels of single-aggregate genes were roughly estimated by the RPKM values of the mapped gene transcripts in the metatranscriptome.

Results and discussion

Genomic and transcriptomic data analysis

The AOM enrichment investigated in this study contains ANME-2a as the dominant archaeal group (Zhang *et al.*, 2011), mainly in the form of aggregates (Supplementary Figure S1). A few cell aggregates were captured from the enrichment, with their DNA isolated, amplified and sequenced as described in the Materials and methods. One captured single aggregate named M25 was found to have ANME-2a as the sole archaeal group with no bacterial partners: no bacterial 16S rRNA gene fragments were amplified, and only ANME-2a 16S rRNA gene was retrieved by archaeal 16S rRNA gene amplification (for details see Materials and methods). M25 was then subjected to in-depth genomic sequencing. Initially, 11 111 112 reads with a length of 90 bp were generated for this single-aggregate genome M25, and resulted in 3.64 Mbp of assembly (Supplementary Table S2). No bacterial 16S rRNA gene fragments were detected from the M25 assembly, and only one 16S rRNA gene sequence assigned to ANME-2a was found (with its phylogeny displayed in Supplementary Figure S2). Meanwhile, as demonstrated in the phylogeny of the methyl-coenzyme M reductase subunit A (McrA, a key enzyme for methane production and oxidation), *mcrA* retrieved from the M25 genome was also assigned to the ANME-2a subgroup (Supplementary Figure S3). The genomic evidences (the annotated 16S rRNA gene and *mcrA* analysis, the absence of bacterial marker genes for sulfate reduction) together with the direct 16S rRNA gene amplification confirmed that M25 contained only ANME-2a without bacterial partners. The genome size for our ANME-2a is estimated to be 3.96 Mbp, with a recovery of ~90% by the current M25 assembly (Supplementary Figure S4, see conserved archaeal single copy gene analysis in Materials and methods). Based on the results of blastx (see taxonomic assignment in Materials and methods), all the genes discussed in this study (as listed in Table 1 and Supplementary Tables S3 and S4) were assigned to Methanosarcinales, where ANME-2a belongs. At present, our understanding on these yet uncultivated ANME-2 genome is limited to a few studies: 11 ANME-2a originated fosmids, totaling ~367 Kb sequence data (Hallam *et al.*, 2004); short sequence read on ANME-2c of 99 bp each (~380 Kb in total) (Pernthaler *et al.*, 2008); and a recently near completed genome for ANME-2d (with a genome size of 3.2 Mbp) capable of methane oxidization coupled to nitrate reduction (Haroon *et al.*, 2013). The genomic data on ANME-2a reported here will improve our understanding on the molecular mechanisms of AOM substantially.

The metatranscriptome of the enrichment contained 1.50E+07 sequence reads, 2262.9 Mb of sequences, and 43.3% of which were non-rRNA thus used for further analysis. Approximately 45% of all non-rRNA transcripts in the metatranscriptome were of archaeal origin (determined by MEGAN+blastx results), and the majority (57%) of these archaeal sequences showed highest similarities to Methanosarcinales. The above data sets were exploited to a detailed investigation on the methane metabolizing pathway in ANME-2a (Table 1 and Supplementary Tables S3 and S4).

Methane-oxidizing pathway

As shown in Table 1, all genes that encode enzymes responsible for the seven central steps in the methanogenic pathway have been identified in the single-aggregate M25 genome and have corresponding transcripts in the metatranscriptome. Our previous activity tests on the same enrichment have proven that the sulfate reduction is dependent on methane oxidation and no methane production was observed when methane was eliminated from the medium (Zhang *et al.*, 2010). ANME-2a is demonstrated to have all the required genes for a complete methane-oxidizing pathway from CH_4 to CO_2 following reversed-methanogenesis hypothesis, and all these genes were actively expressed during the cultivation (Figure 1 and Table 1). Although we cannot completely rule out the possibility of methane productions by ANME-2a under certain conditions (such as the *in situ* environmental conditions), under the controlled incubation condition where

Table 1 Identification of methanogenesis-associated genes in the ANME-2a enrichment sample

Step	*Gene name*	*Abbreviation*	*M25 scaffold ID*	*Transcriptome*
1	*Methyl-coenzyme M reductase subunit A*	*mcrA*	65	2409
	Subunit B	*mcrB*	65	4618
	Subunit C	*mcrC*	65	4112
	Subunit D	*mcrD*	65	3943
	Subunit G	*mcrG*	65	3112
2	*Tetrahydromethanopterin S-methyltransferase subunit A*	*mtrA*	84, 11	1429, 230
	Subunit B	*mtrB*	84, 11	608, NM
	Subunit C	*mtrC*	84, 11	5359, NM
	Subunit D	*mtrD*	84, 11	5080, 173
	Subunit E	*mtrE*	84, 11	6057, 5128
	Subunit F	*mtrF*	84, 11	2948, NM
	Subunit G	*mtrG*	84, 11	470, 50
	Subunit H	*mtrH*	84, 11	1720, 167
3	*Coenzyme F420-dependent N5N10-methylene tetrahydromethanopterinreductase*	*mer1*	5	2652
		mer2	11	393
4	*Methylenetetrahydromethanopterin dehydrogenase*	*mtd*	272	66
5	*Methenyltetrahydromethanopterincyclohydrolase*	*mch*	13	4872
6	*Formylmethanofurantetrahydromethanopterin N-formyltransferase*	*ftr*	1, 1	1581, NM
7	*Formylmethanofuran dehydrogenase subunit A*	*fmdA*	95, 243	6030, NM
	Subunit B	*fmdB*	95	3030
	Subunit C	*fmdC*	95, 243	7392, 7392
	Subunit D	*fmdD*	95, 243	4536, NM
	Subunit E	*fmdE*	NI	NM
	Subunit F	*fmdF*	225	346
	Subunit G	*fmdG*	84	193
	Subunit H	*fmdH*	NI	NM

Abbreviations: NI, not identified; NM, no mapping (transcripts to this SCA gene).Numbers in M25 represent the scaffold ID of the aggregate genome assemblies, and numbers in transcriptome column represent the RPKM (reads per Kb per million reads) value of each gene.

the enrichment was generated, methane oxidation instead of methane production is solely observed.

From our M25 assembly, two complete *mer* genes were identified with 49% sequence identity and designated as *mer-1* and *mer-2*. Phylogenetic analysis of Mer clearly showed a vertical transfer of *mer* gene sequences within different orders of methanogenic archaea (Figure 2). The gene *mer-1* clustered closely with that from ANME-2d (Haroon *et al.*, 2013), classified within the Methanosarcinales, to which ANME-2 belongs, whereas *mer-2* substantially differed from *mer* genes of all known methanogenic archaea. The phylogenetic position of *mer-2* is still unclear, it may come from an unknown archaeon through horizontal gene transfer. The *mer*-1 gene was adjacent to *fpoF* (the gene encoding F_{420}-phenazine oxidoreductase subunit F). This type of gene organization is conserved in *Methanosarcina* species (Baumer *et al.*, 2000; Kulkarni *et al.*, 2009) (Supplementary Figure S5). The finding of canonic *mer* is suggesting that the conversion of methyl-H_4MPT to methylene-H_4MPT in ANME-2 is the reversal of the corresponding reaction operating forward in methanogenesis; the same reversal reaction was not identified in ANME-1 (Hallam *et al.*, 2004; Meyerdierks *et al.*, 2010). The *mer*-2 gene was adjacent to one of two copies of *mtr* (the gene encoding tetrahydromethanopterin *S*-methyltransferase), which was designated as *mtr*-2 (Supplementary Figure S6). The whole sequence identity between two *mtr sets* is ~40%, with the highest identity (45%) found between *mtrA* and the lowest (27%) between *mtrC*. Considering the low sequence similarity between the two sets of *mtr* genes, it is unlikely that one set of the *mtr* genes is an artifact resulting from MDA. The Mtr methyltransferase complex MtrA-H catalyzes methyl transfer from N5-methyltetrahydromethanopterin (or N5-methyltetrahydrosarcinapterin) to coenzyme M in methanogenic archaea (Thauer, 1998). The presence of two sets of *mer* and *mtr* in this ANME-2a is intriguing and, to our knowledge, there is no report of an organism possessing two *mtr* complex sets. It is still a question of whether these two sets of *mer* and *mtr* come from a single organism, as M25 contained multiple cells that may have undertaken extensive genomic differentiation. Nevertheless, the data presented here demonstrate that ANME-2a archaeal group harbors two sets of *mer* and *mtr* genes. The expression levels of *mer*-1 and *mtr-1* were nearly one order of magnitude higher than the expression levels of *mer*-2 and *mtr*-2, respectively, as evaluated by the gene expression RPKM values (Table 1), suggesting a major role of *mer-1* and *mtr-1* in methane oxidation. It remains unclear whether *mer-2* and *mtr-2* take part in the same enzymatic reactions as *mer-1* and *mtr-1* or have other functions and why ANME-2a maintains an additional set of these genes.

H_2-independent energy-converting mechanisms

No canonical hydrogenase was found in either genomic or transcriptomic data, and thus ANME-2a from our

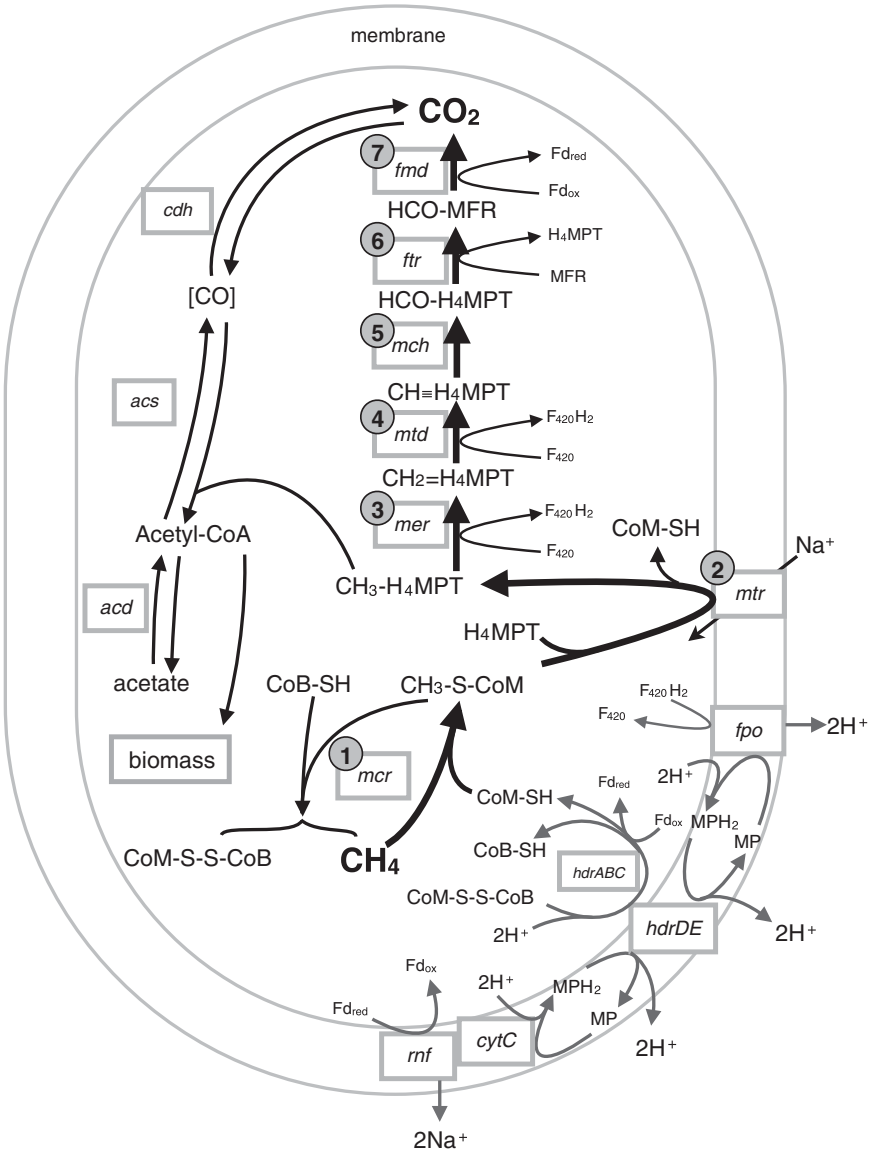

Figure 1 The proposed methane-oxidizing pathway and energy-converting mechanisms in ANME-2a. Only positive gene identifications were displayed (in boxes). The carbon flow was demonstrated with black arrows; the electron flow was indicated with grey arrows. Detailed information of methanogenesis-associated genes is displayed in Table 1, and the names of genes involved in electron transport are displayed in Supplementary Table S3.

enrichment is most probably performing AOM without H_2 as the intracellular electron carrier or intercellular electron shuttle to SRB. Instead, all of the components in the energy-conserving electron transport pathways of non-H_2-utilizing methanogenic archaea, in particular genes for the membrane-associated Coenzyme B–Coenzyme M heterodisulfide reductase HdrDE, genes for CytC (cytochrome *c*) and genes for the Rnf (Rhodobacter nitrogen fixation) complex, which are missing in the H_2-utilizing species, are all identified and expressed in ANME-2a (Supplementary Table S3). Therefore, versatile electron transfer pathways independent of H_2 are postulated within ANME-2a cells. Redox components F_{420}/ $F_{420}H_2$ (the oxidized/reduced forms of a 5′deazaflavin derivative with high concentrations in methanogenic archaea), Fd_{ox}/Fd_{red} (the oxidized/reduced forms of ferredoxin) and MP/MPH_2 (the oxidized/reduced forms of membrane-soluble methanophenazine (MP)) can be recycled to couple methane oxidation with adenosine triphosphate (ATP) synthesis through multiple pathways (Figure 1). For example, the oxidation of $F_{420}H_2$ can be completed via the $F_{420}H_2$:heterodisulfide oxidoreductase system while reducing CoM-S-S-CoB, comprising membrane-bound HdrDE and Fpo, as commonly found in *Methanosarcina* (Baumer *et al.*, 2000; Deppenmeier and Mueller, 2008; Kulkarni *et al.*, 2009). Similarly, Fd_{red}/Fd_{ox} is cycled via a Fd_{red}:heterodisulfide oxidoreductase

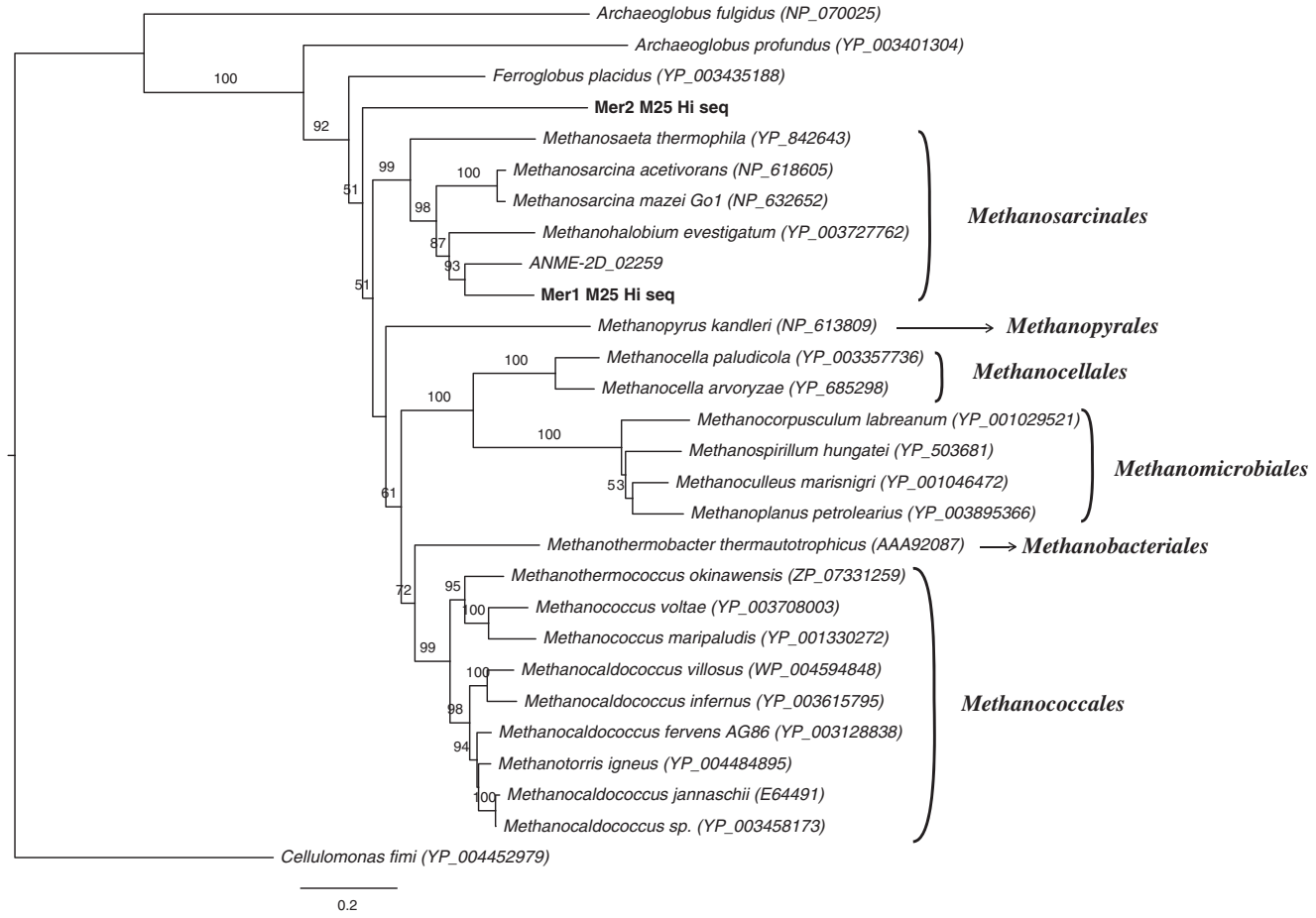

Figure 2 The maximum likelihood tree showing the deduced amino acid sequences of *mer*-1 and *mer*-2 genes to the selected reference sequences. A total of 25 full-length amino acid sequences of *mer* were aligned. Bootstrap values were based on 1000 replicates and shown at the nodes. Mer-1 and Mer-2 from M25 identified in the single-aggregate genome were highlighted, with their detailed information displayed in Table 1.

system including CytC, the Rnf complex and HdrDE that results in a sodium gradient that is exchanged for a proton gradient (Ferry and Lessner, 2008; Wang *et al.*, 2011). This is in agreement with the previous studies that the electron transport pathways in non-H_2-utilizing marine methanogenic species of the *Methanosarcina* genus are fundamentally distinct from those in H_2-utilizing freshwater species (Guss *et al.*, 2009). For example, the non-H_2-utilizing, marine methanogen *Methanosarcina acetivorans* replaces the Ech hydrogenase with the Rnf complex to generate a transmembrane ion gradient for ATP synthesis, which has been interpreted as an adaptation strategy of this species to the marine environment (Wang *et al.*, 2011). In addition, cytoplasmic HdrABC, another type of heterodisulfide reductase, has been detected with multiple copies (Supplementary Table S3). From the phylogenetic analysis, our ANME-2a-originated *hdrA* genes were placed into clades with methyltrophic or/and acetoclastic methanogenic archaea but not H_2-dependent methanogenic archaea (Supplementary Figure S7) (Buan and Metcalf, 2010). We note here that the identified electron transport components HdrDE and the Rnf complex in ANME-2a have not been reported in ANME-1 metagenomes (Hallam *et al.*, 2004; Meyerdierks *et al.*, 2010), indicating that the methane-oxidizing archaea ANME-1 and ANME-2 may have evolved distinct electron transport pathways or strategies, which warrant detailed investigations in the future.

Acetate-metabolizing possibility

Interestingly, Acd (ADP-forming acetyl-CoA synthetase), a recently identified enzyme in archaea that catalyzes the conversion of acetyl-CoA to acetate coupled with the conversion of ADP to ATP ($\text{acetyl-CoA} + \text{ADP} + \text{P}_\text{i} \rightarrow \text{acetate} + \text{ATP} + \text{CoA}$) (Brasen *et al.*, 2008), was detected in the single-aggregate genome and the metatranscriptome (Supplementary Table S4). This finding supports the possible integration of acetate to acetyl-CoA at the cost of ATP before entering reverse methanogenesis and/or biomass synthesis. As a corollary, if acetate from acetyl-CoA is excreted, it could be utilized by SRB. The potential for ANME-2a to metabolize acetate is further supported by its possession of an

Rnf complex in the energy-converting system that has only been found in non-H_2-utilizing acetoclastic *Methanosarcinas* species (Ferry and Lessner, 2008; Wang *et al.*, 2011). The utilization of acetate as an intermediate contradicts results obtained from *in vitro* experiments (Nauhaus *et al.*, 2005), but is consistent with extreme ^{13}C depletion in acetate with $\delta^{13}C$ values approaching $-90‰$ in some methane seep sediments (Heuer *et al.*, 2006). The possibility that the ANME-2a from our enrichment utilizes other methylated C1 compounds such as methylamines or methylsulfides for AOM (Moran *et al.*, 2008) is not supported by this study (Supplementary Table S4).

Ecological and evolutionary implications

Although we cannot entirely rule out the potential presence of hydrogenase because of incompleteness of our current ANME-2a genome, the results from this study suggest that the interspecies hydrogen transfer does not play a major role in forming syntrophic consortia of ANME-2a and bacteria in cold seep ecosystems. It is commonly assumed that interspecies electron transfer is a key process in shaping syntrophic communities, especially in methanogenic, anaerobic methanotrophic, sulfate-reducing and even subsurface ecosystems (Nealson *et al.*, 2005; Stams and Plugge, 2009). The utilization of H^+/H_2 as the electron shuttle is facilitated by the relatively easy transfer of protons and the lacking requirement of enzymes with complex active centers (Vignais and Billoud, 2007). On the other hand, the low midpoint redox potential of this redox couple ($E^\circ = -414\,mV$, which is lower than those of $NAD^+/NADH$, $FADH/FADH_2$, Fd_{ox}/Fd_{red}) causes an energetic problem unless hydrogen is continuously produced and removed by two distinct organisms. A recent publication described a mechanism in which zero-valent sulfur produced via sulfate reduction by ANME-2 served as intermediate for an ANME/SRB syntrophic community and was disproportionated by SRB (Milucka *et al.*, 2012). It needs to be tested in the future whether sulfur/acetate rather than H_2 serves as electron shuttle between ANME-2a and its SRB partner.

This report demonstrates that ANME-2a oxidizes methane to CO_2 with genes from versatile electron transport pathways that do not likely involve H_2, and that ANME-2a possesses the potential ability to produce and utilize acetate. It is shown that ANME-2a in our enrichment clearly shares similarities with members of the Methanosarcinales, in particular with non-H_2-utilizing acetoclastic *Methanosarcina* species. Both ANME-2 and *Methanosarcina* contain cytochrome and MP and they perform complete reverse or forward methanogenesis respectively, while generating ATP without hydrogenase. These features directly reveal a close evolutionary relationship between ANME-2 and the Methanosarcinales and reflect the natural habitat of ANME-2. As the only order of methanogenic archaea with cytochromes, Methanosarcinales requires a higher threshold of H_2 partial pressure to produce methane from H_2 and CO_2 compared with methanogenic archaea without cytochromes. Therefore, some species from Methanosarcinales, including the ancestors of ANME-2, may have lost the ability to metabolize H_2, whereas most species can grow on acetate and C1 compounds (Bonin and Boone, 2006). In addition, compared with methanogenic archaea from fresh water, marine isolates tend to forego H_2-dependent electron transport pathways to outcompete with other organisms because of the easy loss of freely diffusible H_2 gas within marine environments (Guss *et al.*, 2005). Moreover, the possession of cytochromes constrains Methanosarcinales to habitats colder than 60 °C, that is, a temperature above which their growth is energetically unfavorable (Conrad and Wetter, 1990; Kotsyurbenko *et al.*, 2001). This is consistent with the finding that ANME-2 preferentially inhabits in low-temperature settings, whereas ANME-1 is widely distributed even in high-temperature environments such as hydrothermal vents (Holler *et al.*, 2011; Rossel *et al.*, 2011; Biddle *et al.*, 2012). Furthermore, genes involved in a broad substrate utilization spectrum and versatile energy-converting mechanisms are expressed in ANME-2, highlighting the flexibility of ANME-2 to adjust to fluctuating environments with intermittently high redox potentials, such as sporadically oxygenated shallow marine sediments (Knittel *et al.*, 2005; Lazar *et al.*, 2011; Rossel *et al.*, 2011).

Our study of an ANME-2a enrichment demonstrated that its methane-oxidizing and electron-transporting pathways are distinct from ANME-1 and advanced our understanding on the globally relevant AOM biogeochemical process. These results have important implications for the evolution, physiology and niche differentiation of different ANME clades.

Conflict of Interest

The authors declare no conflict of interest.

Acknowledgements

This work was supported by the National Basic Research Program of China (2011CB808800), the National Natural Science Foundation of China (91228201, 31290232), the National High-Tech Program (2012AA092103-2), a research fund from the European Science Foundation MicroSYSTEMS supported by Fondsvoor Wetenschappelijk Onderzoek (506G.0656.05) and a research grant from the Geconcerteerde Onderzoeks actie (GOA) of Ghent University (BOF09/GOA/005). We sincerely thank Professor Rudolf K Thauer for his critical review and constructive advice for improving this manuscript.

References

Altschul SF, Madden TL, Schaffer AA, Zhang J, Zhang Z, Miller W *et al.* (1997). Gapped BLAST and PSI-BLAST: a new generation of protein database search programs. *Nucleic Acids Res* **25**: 3389–3402.

Baumer S, Ide T, Jacobi C, Johann A, Gottschalk G, Deppenmeier U. (2000). The F420H2 dehydrogenase from Methanosarcina mazei is a redox-driven proton pump closely related to NADH dehydrogenases. *J Biol Chem* **275**: 17968–17973.

Biddle JF, Cardman Z, Mendlovitz H, Albert DB, Lloyd KG, Boetius A *et al.* (2012). Anaerobic oxidation of methane at different temperature regimes in Guaymas Basin hydrothermal sediments. *ISME J* **6**: 1018–1031.

Boetius A, Ravenschlag K, Schubert CJ, Rickert D, Widdel F, Gieseke A *et al.* (2000). A marine microbial consortium apparently mediating anaerobic oxidation of methane. *Nature* **407**: 623–626.

Bonin AS, Boone DR. (2006). *The Order Methanobacteriales*. Springer: New York.

Brasen C, Schmidt M, Grotzinger J, Schonheit P. (2008). Reaction mechanism and structural model of ADP-forming acetyl-CoA synthetase from the hyperthermophilic archaeon Pyrococcus furiosus - evidence for a second active site histidine residue. *J Biol Chem* **283**: 15409–15418.

Buan NR, Metcalf WW. (2010). Methanogenesis by Methanosarcina acetivorans involves two structurally and functionally distinct classes of heterodisulfide reductase. *Mol Microbiol* **75**: 843–853.

Conrad R, Wetter B. (1990). Influence of temperature on energetics of hydrogen metabolism in homoacetogenic, methanogenic, and other anaerobic bacteria. *Arch Microbiol* **155**: 94–98.

Delcher AL, Bratke KA, Powers EC, Salzberg SL. (2007). Identifying bacterial genes and endosymbiont DNA with Glimmer. *Bioinformatics* **23**: 673–679.

Delong EF. (1992). Archaea in coastal marine environments. *Proc Natl Acad Sci USA* **89**: 5685–5689.

Deppenmeier U, Mueller V. (2008). Life close to the thermodynamic limit: how methanogenic archaea conserve energy. In: Schafer G, Penefsky HS (eds) *Results and Problems in Cell Differentiation*. Springer-Verlag: Berlin, pp 123–152.

Ferry JG, Lessner DJ. (2008). Methanogenesis in marine sediments. In: Wiegel J, Maier RJ, Adams MWW (eds) *Incredible Anaerobes: From Physiology to Genomics to Fuels*. Blackwell Publishing: Oxford, pp 147–157.

Guindon S, Gascuel O. (2003). A simple, fast, and accurate algorithm to estimate large phylogenies by maximum likelihood. *Syst Biol* **52**: 696–704.

Guss AM, Mukhopadhyay B, Zhang JK, Metcalf WW. (2005). Genetic analysis of mch mutants in two Methanosarcina species demonstrates multiple roles for the methanopterin-dependent C-1 oxidation/reduction pathway and differences in H-2 metabolism between closely related species. *Mol Microbiol* **55**: 1671–1680.

Guss AM, Kulkarni G, Metcalf WW. (2009). Differences in hydrogenase gene expression between Methanosarcina acetivorans and Methanosarcina barkeri. *J Bacteriol* **191**: 2826–2833.

Hallam SJ, Putnam N, Preston CM, Detter JC, Rokhsar D, Richardson PM *et al.* (2004). Reverse methanogenesis: testing the hypothesis with environmental genomics. *Science* **305**: 1457–1462.

Haroon MF, Hu S, Shi Y, Imelfort M, Keller J, Hugenholtz P *et al.* (2013). Anaerobic oxidation of methane coupled to nitrate reduction in a novel archaeal lineage. *Nature* **500**: 567–570.

Heuer V, Elvert M, Tille S, Krummen M, Mollar XP, Hmelo LR *et al.* (2006). Online delta C-13 analysis of volatile fatty acids in sediment/porewater systems by liquid chromatography-isotope ratio mass spectrometry. *Limnol Oceanogr Meth* **4**: 346–357.

Hinrichs KU, Hayes JM, Sylva SP, Brewer PG, DeLong EF. (1999). Methane-consuming archaebacteria in marine sediments. *Nature* **398**: 802–805.

Hoehler TM, Alperin MJ, Albert DB. (1994). Field and laboratory studies of methane oxidation in an anoxic marine sediment: evidence for a methanogen-sulfate reducer consortium. *Global Biogeochem Cy* **8**: 451–463.

Holler T, Widdel F, Knittel K, Amann R, Kellermann MY, Hinrichs KU *et al.* (2011). Thermophilic anaerobic oxidation of methane by marine microbial consortia. *ISME J* **5**: 1946–1956.

Huang Y, Gilna P, Li WZ. (2009). Identification of ribosomal RNA genes in metagenomic fragments. *Bioinformatics* **25**: 1338–1340.

Huson D, Auch A, Qi J, Schuster S. (2007). MEGAN analysis of metagenomic data. *Genome Res* **17**: 377–386.

Knittel K, Losekann T, Boetius A, Kort R, Amann R. (2005). Diversity and distribution of methanotrophic archaea at cold seeps. *Appl Environ Microbiol* **71**: 467–479.

Knittel K, Boetius A. (2009). Anaerobic oxidation of methane: progress with an unknown process. *Annu Rev Microbiol* **63**: 311–334.

Kotsyurbenko OR, Glagolev MV, Nozhevnikova AN, Conrad R. (2001). Competition between homoacetogenic bacteria and methanogenic archaea for hydrogen at low temperature. *FEMS Microbiol Ecol* **38**: 153–159.

Kulkarni G, Kridelbaugh DM, Guss AM, Metcalf WW. (2009). Hydrogen is a preferred intermediate in the energy-conserving electron transport chain of Methanosarcina barkeri. *Proc Natl Acad Sci USA* **106**: 15915–15920.

Larkin MA, Blackshields G, Brown NP, Chenna R, McGettigan PA, McWilliam H *et al.* (2007). Clustal W and Clustal X version 2.0. *Bioinformatics* **23**: 2947–2948.

Lazar CS, Dinasquet J, L'Haridon S, Pignet P, Toffin L. (2011). Distribution of anaerobic methane-oxidizing and sulfate-reducing communities in the G11 Nyegga pockmark, Norwegian Sea. *Antonie Van Leeuwenhoek* **100**: 639–653.

Li R, Yu C, Li Y, Lam TW, Yiu SM, Kristiansen K *et al.* (2009). SOAP2: an improved ultrafast tool for short read alignment. *Bioinformatics* **25**: 1966–1967.

Markowitz VM, Chen IM, Palaniappan K, Chu K, Szeto E, Grechkin Y *et al.* (2012). IMG: the Integrated Microbial Genomes database and comparative analysis system. *Nucleic Acids Res* **40**: D115–D122.

Meyerdierks A, Kube M, Kostadinov I, Teeling H, Glockner FO, Reinhardt R *et al.* (2010). Metagenome and mRNA expression analyses of anaerobic methanotrophic archaea of the ANME-1 group. *Environ Microbiol* **12**: 422–439.

Milucka J, Ferdelman TG, Polerecky L, Franzke D, Wegener G, Schmid M *et al.* (2012). Zero-valent sulphur is a key intermediate in marine methane oxidation. *Nature* **491**: 541–546.

Moran JJ, Beal EJ, Vrentas JM, Orphan VJ, Freeman KH, House CH. (2008). Methyl sulfides as intermediates in the anaerobic oxidation of methane. *Environ Microbiol* **10**: 162–173.

Mortazavi A, Williams BA, McCue K, Schaeffer L, Wold B. (2008). Mapping and quantifying mammalian transcriptomes by RNA-Seq. *Nat Meth* **5**: 621–628.

Nauhaus K, Treude T, Boetius A, Kruger M. (2005). Environmental regulation of the anaerobic oxidation of methane: a comparison of ANME-I and ANME-II communities. *Environ Microbiol* **7**: 98–106.

Nealson KH, Inagaki F, Takai K. (2005). Hydrogen-driven subsurface lithoautotrophic microbial ecosystems (SLiMEs): do they exist and why should we care? *Trends Microbiol* **13**: 405–410.

Noguchi H, Taniguchi T, Itoh T. (2008). MetaGeneAnnotator: detecting species-specific patterns of ribosomal binding site for precise gene prediction in anonymous prokaryotic and phage genomes. *DNA Res* **15**: 387–396.

Ogata H, Goto S, Sato K, Fujibuchi W, Bono H, Kanehisa M. (1999). KEGG: Kyoto Encyclopedia of Genes and Genomes. *Nucleic Acids Res* **27**: 29–34.

Orphan VJ, Hinrichs KU, Ussler W, Paull CK, Taylor LT, Sylva SP *et al.* (2001). Comparative analysis of methane-oxidizing archaea and sulfate-reducing bacteria in anoxic marine sediments. *Appl Environ Microbiol* **67**: 1922–1934.

Pernthaler A, Dekas AE, Brown CT, Goffredi SK, Embaye T, Orphan VJ. (2008). Diverse syntrophic partnerships from-deep-sea methane vents revealed by direct cell capture and metagenomics. *Proc Natl Acad Sci USA* **105**: 7052–7057.

Pruesse E, Quast C, Knittel K, Fuchs BM, Ludwig W, Peplies J *et al.* (2007). SILVA: a comprehensive online resource for quality checked and aligned ribosomal RNA sequence data compatible with ARB. *Nucleic Acids Res* **35**: 7188–7196.

Reeburgh WS. (1976). Methane consumption in Cariaco Trench waters and sediments. *Earth Planet Sc Lett* **28**: 337–344.

Reeburgh WS. (2007). Oceanic methane biogeochemistry. *Chem Rev* **107**: 486–513.

Rossel PE, Elvert M, Ramette A, Boetius A, Hinrichs KU. (2011). Factors controlling the distribution of anaerobic methanotrophic communities in marine environments: evidence from intact polar membrane lipids. *Geochim Cosmochim Acta* **75**: 164–184.

Stahl DA, Amann R. (1991). Development and application of nucleic acid probes. In: Stackebrandt E, Goodfellow M (eds) *Nucleic Acid Techniques in Bacterial Systematics*. John Wiley & Sons: Chichester, pp 205–248.

Stams AJM, Plugge CM. (2009). Electron transfer in syntrophic communities of anaerobic bacteria and archaea. *Nat Rev Microbiol* **7**: 568–577.

Stokke R, Roalkvam I, Lanzen A, Haflidason H, Steen IH. (2012). Integrated metagenomic and metaproteomic analyses of an ANME-1-dominated community in marine cold seep sediments. *Environ Microbiol* **14**: 1333–1346.

Tatusov RL, Galperin MY, Natale DA, Koonin EV. (2000). The COG database: a tool for genome-scale analysis of protein functions and evolution. *Nucleic Acids Res* **28**: 33–36.

Thauer RK. (1998). Biochemistry of methanogenesis: a tribute to Marjory Stephenson. *Microbiology* **144**: 2377–2406.

Thauer RK. (2011). Anaerobic oxidation of methane with sulfate: on the reversibility of the reactions that are catalyzed by enzymes also involved in methanogenesis from CO2. *Curr Opin Microbiol* **14**: 292–299.

Treude T, Knittel K, Blumenberg M, Seifert R, Boetius A. (2005). Subsurface microbial methanotrophic mats in the Black Sea. *Appl Environ Microbiol* **71**: 6375–6378.

Vignais PM, Billoud B. (2007). Occurrence, classification, and biological function of hydrogenases: an overview. *Chem Rev* **107**: 4206–4272.

Wang M, Tomb JF, Ferry JG. (2011). Electron transport in acetate-grown Methanosarcina acetivorans. *BMC Microbiol* **11**: 165.

Woyke T, Xie G, Copeland A, Gonzalez JM, Han C, Kiss H *et al.* (2009). Assembling the marine metagenome, one cell at a time. *PLoS One* **4**: e5299.

Zhang Y, Henriet JP, Bursens J, Boon N. (2010). Stimulation of in vitro anaerobic oxidation of methane rate in a continuous high-pressure bioreactor. *Bioresour Technol* **101**: 3132–3138.

Zhang Y, Maignien L, Zhao X, Wang F, Boon N. (2011). Enrichment of a microbial community performing anaerobic oxidation of methane in a continuous high-pressure bioreactor. *BMC Microbiol* **11**: 137.

Supplementary Information accompanies this paper on The ISME Journal website (http://www.nature.com/ismej)